Progress In Electromagnetics Research, PIER 102, 301–313, 2010

WIDE-BAND HYBRID AMPLIFIER OPERATING IN S-BAND REGION

S. D. Emami

Department of Electrical Engineering
University of Malaya
50603 Kuala Lumpur, Malaysia

P. Hajireza

Faculty of Engineering
Multimedia University
63100 Cyberjaya, Malaysia

F. Abd-Rahman

Department of Electrical and Electronic Engineering
Universiti Tunku Abdul Rahman
Kuala Lumpur, Malaysia

H. A. Abdul-Rashid

Faculty of Engineering
Multimedia University
63100 Cyberjaya, Malaysia

H. Ahmad

Photonics Research Center
University of Malaya
50603 Kuala Lumpur, Malaysia

S. W. Harun †

Department of Electrical Engineering
University of Malaya
50603 Kuala Lumpur, Malaysia

Corresponding author: S. W. Harun (swharun@um.edu.my).

† Also with Photonics Research Center, University of Malaya, 50603 Kuala Lumpur, Malaysia.

Abstract—Wide-band hybrid amplifier is theoretically proposed using a series configuration of Thulium-doped fiber amplifier (TDFA) and fiber Raman amplifier (FRA), which using the similar type of pump laser. The operating wavelength of this amplifier covers the bandwidth of entire short wavelength band (S-band) region by combining the gain spectrum of TDFA and FRA. The theoretical gain varies from 20 to 24 dB within a wavelength region from 1460 to 1525 nm and which is in a good agreement with the experimental result. The development of reliable high-power diode lasers in the 1420 nm wavelength range will make this type of wide-band hybrid amplifier an interesting candidate for S-band optical telecommunication systems.

1. INTRODUCTION

Recently, many research works have been focused on the fiber-optic devices for optical communication systems [1–7]. One of the main interests is on the optical amplifiers to boost a weak signal in the communication systems [8–10]. One of the effective ways to extend the gain bandwidth of the optical amplifiers is to use a hybrid amplifier that combines several amplifiers with different gain bandwidths. Connecting two different amplifiers in parallel or in series are some of the methods used to achieve a wide-band amplifier [10]. In case of parallel configuration, the input signal is firstly de-multiplexed into different band by the wavelength division multiplexing (WDM) coupler, amplified by amplifiers that are suitable for the corresponding wavelength band, and finally multiplexed again with a WDM coupler. This type of hybrid amplifier has the advantage of extensibility, in which one amplifier can initially work independently while another amplifier can be added into the system according to the capacity demand expansion. Unusable wavelength region exists between each gain band originated from the guard band of the WDM coupler is the main disadvantages of the parallel type of hybrid amplifier. The noise figure of this amplifier also increases due to the insertion loss of the WDM coupler, which is located at the input end of each amplifier. To cope with this problem, the hybrid amplifier can be connected in series to avoid the use of the WDM coupler [11].

Due to the tremendous increase in communication traffic in recent years, more and more efforts in research have been directed towards developing highly efficient fiber amplifiers that operates in short wavelength band (S-band) region. Thulium-doped fiber amplifier (TDFA) and fiber Raman amplifier (FRA) are two promising candidates for the S-band amplifiers [12, 13]. In an earlier work,

Kani and Jinno proposed a wide-band optical amplifier by serially connecting a TDFA and FRA [14]. The TDFA and FRA were pumped by a laser diode operating at 1047 nm and 1415 nm respectively. In this paper, a hybrid amplifier operating in S-band region is proposed based on a similar approach but using a 1420 nm pump laser to pump both linear and nonlinear gain media. The theoretical analysis of the hybrid amplifier is developed to investigate the gain and noise figure performance. The theoretical results are also compared and verified with the experimental results.

2. THEORETICAL ANALYSIS

2.1. Thulium-doped Fiber Amplifier with 1420 nm Pumping

Figure 1 shows the energy level diagram of the TDFA in low-phonon-energy fluoride glasses, which demonstrates both radiative and non-radiative transitions. The variables N_0, N_1, N_2 and N_3 are used to represent population of ions in the $^3H_6$, $^3F_4$, $^3H_5$ and $^3H_4$ energy levels respectively. The S-band amplification is due to the population inversion between the $^3H_4$ and $^3F_4$ energy levels. The stimulated emission from the $^3H_4$ to $^3F_4$ level emits photons at wavelength region from 1380 to 1550 nm with a peak at 1460 nm [15]. Based on Fig. 1, the rate equation for the ion population at each layer of TDFA can be

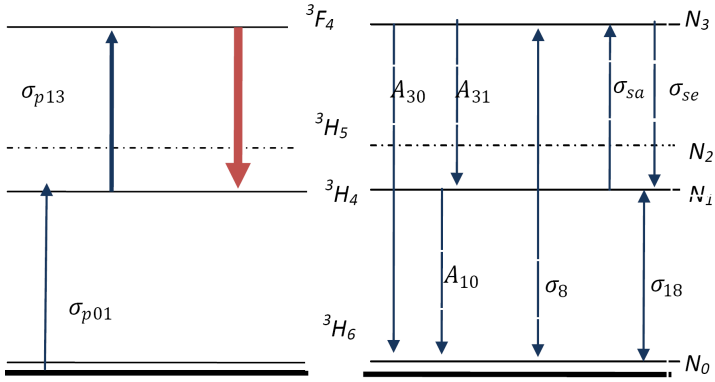

Figure 1. Pumping mechanism of a 1420 nm pumped TDFA. (a) Absorption or pump transitions. (b) Signal and ASE emission transitions.

written as;

$$\frac{dN_0}{dt}=-(W_{p01}+W_{18a}+W_{8a})N_0+(A_{10}+W_{18e})N_1+(A_{30}+W_{8e})N_3 \quad (1)$$

$$\frac{dN_1}{dt}=(W_{18a}+W_{p01})N_0-(A_{10}+W_{p13}+W_{Sa}+W_{18e})N_1 +(W_{p31}+W_{Se}+A_{31})N_3 \quad (2)$$

$$\frac{dN_3}{dt}=(W_{8a})N_0+(W_{p13}+W_{Sa})N_1 -(A_{30}+A_{31}+W_{p31}+W_{se}+W_{8e})N_3 \quad (3)$$

$$\sum\nolimits_i N_i=\rho \quad (4)$$

where W_{p01}, W_{p13} and W_{p31} are transition rates due to the 1420 nm pumping. Signal stimulated absorption and emission are described by W_{sa} and W_{se} respectively. The transition rates of amplified spontaneous emission (ASE) at 800 nm ($^3H_4 \rightarrow {}^3H_6$) and 1800 nm ($^3F_4 \rightarrow {}^3H_6$) are governed by W_{8e}, W_{18e} respectively. The transition rates of stimulated absorption at 800 nm ($^3H_4 \rightarrow {}^3H_6$) and 1800 nm ($^3F_4 \rightarrow {}^3H_6$) are governed by W_{8a}, W_{18a} respectively. A_{ij} is the radiative rate from level i to level j. Others radiative transitions are not included in the rate equations because they have an ignorable effect on the S-band amplification. Transition rates of the pump, stimulated absorption and stimulated emission are given by:

$$W_{p01,p13,p31} = \lambda_P \sigma_{p01,p13,p31} \left(\frac{P_P^+}{hcA_{eff}} \right) \quad (5)$$

$$W_{8a,8e,18a,18e} = \lambda_{ASE}^{8,18} \sigma_{8a,8e,18a,18e} \left(\frac{P_{ASE}^{8,18+} + P_{ASE}^{8,18-}}{hcA_{eff}} \right) \quad (6)$$

$$W_{sa,se} = \lambda \sigma_{sa,se} \left(\frac{P_{ASE}^+ P_{ASE}^-}{hcA_{eff}} \right) + \lambda_s \sigma_{sa,se} \left(\frac{P_S}{hcA_{eff}} \right) \quad (7)$$

where σ is the absorption cross-section, c is the speed of light in vacuum, h is a plank constant, A_{eff} is the effective area of the thulium-doped fiber (TDF). P_p, P_s and P_{ase} are the pump, signal and ASE powers respectively. The light wave intensity evolution along the doped fiber in the z-direction can be established as follows:

$$\frac{dP_p^{\pm}}{dz} = \mp\Gamma(\lambda_{p1})(\sigma_{p13}N_3 - \sigma_{p01}N_1) \times P_{p1}^{\pm} \mp \alpha P_{p1}^{\pm} \quad (8)$$

$$\frac{dP_s}{dz} = \Gamma(\lambda_s)(\sigma_{se}(\lambda_s)N_3 - \sigma_{sa}(\lambda_s)N_1) \times dP_s - \alpha P_s \quad (9)$$

$$\frac{dP_{ASE}^{\pm}}{dz} = \mp\Gamma(\lambda_{ase})(\sigma_{se}(\lambda_{ase})N_3) - \sigma_{sa}(\lambda_{ase})N_1) \times P_{ASE}^{\pm} \pm\Gamma(\lambda_{ase})(2h\nu\Delta\nu\sigma_{se}(\lambda_{ase})N_3) \mp \alpha P_{ASE}^{\pm} \quad (10)$$

$$\frac{dP_{ASE}^{8\pm}}{dz} = \mp\Gamma(\lambda_8)(\sigma_{8e}(\lambda_8)N_3) - \sigma_{8a}(\lambda_8)N_0) \times P_{ASE}^{8\pm} \pm\Gamma(\lambda_8)(2h\nu\Delta\nu\sigma_8(\lambda_8)N_3) \mp \alpha P_{ASE}^{8\pm} \quad (11)$$

$$\frac{dP_{ASE}^{18\pm}}{dz} = \mp\Gamma(\lambda_{18})(\sigma_{18e}(\lambda_{18})N_1) - \sigma_{18a}(\lambda_{18})N_0) \times P_{ASE}^{18\pm} \pm\Gamma(\lambda_{18})(2h\nu\Delta\nu\sigma_{18}(\lambda_{18})N_1) \mp \alpha P_{ASE}^{18\pm} \quad (12)$$

where α is the background scattering loss, which is assumed to be constant for all wavelengths. λ_{ASE}, λ_{ASE8} and λ_{ASE18} are the signal wavelengths, 800 nm ASE and 1800 nm ASE respectively. The overlapping factors between each radiation and the fiber fundamental mode, $\Gamma(\lambda)$ can be expressed as [16]:

$$\Gamma(\lambda) = 1 - e^{-\frac{2b^2}{\omega_0^2}} \quad (13)$$

$$\omega_0 = a\left(0.761 + \frac{1.237}{V^{1.5}} + \frac{1.429}{V^6}\right) \quad (14)$$

where ω_0 is the mode field radius defined by Equation (14), a is the core diameter, b is the thulium ion-dopant radius and V is the normalized frequency. The noise figure is calculated using the following equation;

$$NF = 1/G + P_{ASE}/(G \times h \times \nu \times \Delta\nu) \quad (15)$$

2.2. FRA with 1420 nm Pumping

In order to obtain Raman amplification, a large pump power must be launched into the gain medium at a shorter wavelength to generate a stimulated Raman scattering (SRS) at a longer wavelength region. Raman gain depends on the amount of pump power and the frequency offset between pump source and signal. Amplification occurs when the pumping photons at the shorter wavelength transfers their energy to new longer wavelength photons. For a single signal, the pump power threshold that is required to achieve the SRS is given by [17]:

$$P_{th} = \frac{16A_{\mathit{eff}}}{K_p L_{\mathit{eff}} g_r} \quad (16)$$

where K_p is the polarization constant which is around 2. A_{eff} and L_{eff} are the effective area and length of SMF fiber respectively. The overall

Raman gain can be expressed in terms of the pump power and pump intensity as

$$g(\nu) = g_r(\nu) I_p = g_r(\nu) \frac{P_p}{A_{eff}} \tag{17}$$

The above equation shows that gain is depending on the pump wavelength and pump power.

The interaction between the forward pump and signal pump as well as a backward pump power and signal power during the SRS process are governed by the following three coupled equations [17];

$$\frac{dP_s}{dz} = \frac{g_r}{A_{eff}} P_p^{\pm} P_s - \alpha_s P_s \tag{18}$$

$$\frac{dP_p^+}{dz} = -\frac{\omega_p}{\omega_s} P_p^+ P_s - \alpha_p P_p^+ \tag{19}$$

$$\frac{dP_p^-}{dz} = \frac{\omega_p}{\omega_s} P_p^- P_s + \alpha_p P_p^- \tag{20}$$

where z is signal propagation direction, A_{eff} is effective area of the Raman fiber as well as α_s and α_p account for fiber losses at signal frequency and pump frequency respectively. These equations describe the pump and signal power transfer along a length of fiber. One of the critical design issues is the Raman gain efficiency which is defined as $g_{R_eff} = g_R / A_{eff}$. The efficiency is depended on the effective areas, material and structure of the gain medium and therefore different fibers will have different gain efficiency. In SRS process, the pump power provides the energy for amplification and depletes as the pump signal propagates along the fiber. Therefore, the gain reduces as the pump signal transfer all of its energy to input signal power, which resulted in gain saturation. The power along the length of the fiber is also reduced by the fiber losses, which occur in the medium due to its intrinsic properties. The pump depletion must be included for complete description of SRS but it is neglected for purpose of estimating the Raman threshold pump power. If the first term on the right hand side of Equations (19) and (20) ignores the pump depletion, then these equations can be summarized as [18, 19]:

$$P_p^+(z) = P_{P_in}^+ e^{-\alpha_p L(z)} \tag{21}$$

$$P_p^-(z) = P_{P_in}^- e^{+\alpha_p L(z)} \tag{22}$$

Here, $P_{P_in}^+$ and $P_{P_in}^-$ is the forward and backward Raman pump powers at the beginning of the transmission fiber respectively. However, in case of bidirectional pumping, the coupled equation can be slightly more complicated because two pump lasers, which are located

at both fiber ends, are used. The pump power evolution in the fiber for the bidirectional FRA is described by [19]:

$$P_p(z) = P_{P_in}\{r_f e^{-\alpha_p L(z)} + (1 + r_f)e^{-\alpha_p(L-L(z))} \tag{23}$$

where r_f is the ratio of the amount pump power launched in forward direction compared to the total pump power and it varies from 0 to 1. Using this equation, the signal intensity evolution in the fiber can also be described as:

$$\frac{dP_s}{dz} = \frac{g_r}{A_{eff}} P^{\pm}_{P_in} e^{-\alpha_{pz}} P_s - \alpha_s P_s \tag{24}$$

By solving this equation, we obtain

$$P_{s(z)} = P_{s_in(z)} e^{\left[\frac{g_R P^{\pm}_{P_{in}}}{A_{eff}(-\alpha_p)}(e^{-\alpha_p z-1}) - \alpha_s z\right]} \tag{25}$$

Hence, the signal intensity at fiber output of length L can be determined as:

$$P_{s(l)} = P_{s_in(0)} e^{\left(\frac{g_R P^{\pm}_0 L_{eff}}{A_{eff}} - \alpha_s z\right)} \tag{26}$$

where L_{eff} is the effective length, which is defined as

$$L_{eff} = \frac{1 - e^{-\alpha_{pL}}}{\alpha_P} \tag{27}$$

Thus, the net Raman gain is calculated as:

$$G(z) = \frac{P_s(z)}{P_s(0)} = \exp(g_R \int_0^z P_p(z)dz - \alpha_s z) \tag{28}$$

Raman gain is defined as the ratio of the power of the signal with and without Raman amplification and it is given by:

$$G_A = e^{Lg_0} \tag{29}$$

where g_0 is small signal gain and is defined as

$$g_0 = \frac{g_R P_0}{A_{eff}\alpha_p L}. \tag{30}$$

Rayleigh scattering is one of the most important phenomena that limit the performance of the FRA. Rayleigh scattering cause small parts of light back scattered. Normally, this Rayleigh back scattering is negligible. However in FRA this scattering may be amplified over a long length of transmission fiber by the Raman pump and affects the amplification performance in two ways. Firstly, double Rayleigh scattering of the signal in optical fiber creates a crosstalk component in the forward direction and secondly, backward propagating noise part

appears in the forward direction and enhancing the noise figure. The noise figure is strongly dependent on the ASE power [17]. The ASE power in the transmission fiber is given by:

$$P_{ASE} = \eta_{sp}(G_r - 1)hV_sB_0 \tag{31}$$

where, h is Planks constant, V_s is signal frequency, B_0 is the electrical bandwidth and η_{sp} is the spontaneous emission and is calculated as:

$$\eta_{sp} = \frac{\eta N_2}{\eta N_2 - N_1} \tag{32}$$

where $\eta = \frac{\sigma_{SE}}{\sigma_{SA}}$. In overall, the noise figure at the signal wavelength λ_s is calculated as:

$$NF(\lambda_s) = \frac{P_{pre}^{ASE}}{(G_r - 1)hV_s\Delta V} \tag{33}$$

3. NUMERICAL CALCULATION

Figure 2 shows the configuration of the proposed hybrid amplifier, in which the TDF and SMF are cascaded in series. The 20 m long TDF and 12 km long SMF are used as the gain medium for the TDFA and FRA, respectively. Both pieces of TDF and SMF are pumped by a 1420 nm pump laser using a forward and bidirectional pumping scheme respectively. 1420 nm/1550 nm wavelength division multiplexing (WDM) couplers are used to combine the 1420 nm laser diode and the pump signal. The theoretical results of TDFA are obtained by solving the rate equations of the pump, signal power

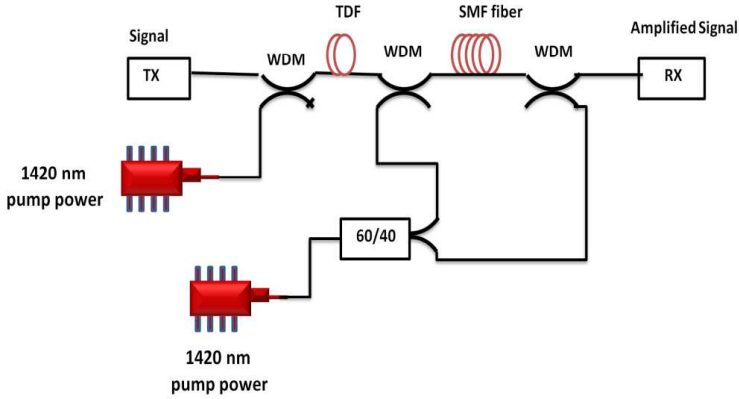

Figure 2. Basic configurations of the hybrid TDFA/FRA.

Table 1. Numerical parameter used in the TDFA's simulation.

Parameter	Unit	Sym	Value
Thulium concentration	$1/m^3$	ρ	1.68×10^2
Numerical aperture		NA	0.3
Fiber Length	m	L	20
Background lost	dB/m	α	1.68×10^2
Effective area	m^2	A_{eff}	2.096×1
Division along fiber			12
800 nm ASE bandwidth	nm	$\Delta\nu_8$	10
1800 nm ASE bandwidth	nm	$\Delta\nu_{18}$	100
ASE bandwidth	nm	$\Delta\nu$	2
Signal absorption cross section	m^2	σ_{sa}	Fig
Signal stimulated emission cross section	m^2	σ_{se}	FIg
800 nm transition cross section	m^2	$\sigma_{03,}$	6.2×10^{-25}
1800 nm transition cross section	m^2	$\sigma_{01,}$	5.2×10^{-25}
Radiative decay rate	1/s	A_{10}	172.4
Radiative decay rate	1/s	A_{30}	702.8
Radiative decay rate	1/s	A_{50}	676.3
Radiative decay rate	1/s	A_{52}	492.9
Nonadiative decay rate	1/s	A_{43}^{nr}	52976
Nonadiative decay rate	1/s	A_{21}^{nr}	165626

Table 2. Numerical parameter used in the FRA's simulation.

Parameter	Unit	Symbol	Value
Numerical aperture		NA	0.3
Fiber Length	km	L	12
Background lost	dB/m	α	1.68×10^{25}
Effective area	m^2	A_{eff}	$70e-12$
Signal wavelength	nm	λs	1550
Pump wavelength	nm	λp	1420
Input signal Power	nm	P_{s_in}	0.1
Raman Gain coefficient	m/W	g_R	$1.0324886e-03$

and ASE using a numerical method. The variables used in the numerical calculation and their corresponding values are shown in Table 1, which is obtained from various publications [15, 20–22]. For FRA simulation, ode45 built in Matlab function was used to solve the numerical equations. The variable used in the numerical calculation and their corresponding values are shown in Table 2.

4. RESULTS AND DISCUSSION

Figure 3 shows the gain spectrum of the proposed hybrid amplifier at total 1480 nm pump power of 800 mW. The theoretical curves are obtained by connecting the numerical gain values, which were calculated from the theoretical analysis at wavelength interval of 0.5 nm. The smoother curve is expected by increasing the number of points. The gain spectra of the individual TDFA and FRA are also shown in Fig. 3 for comparison purpose. The TDF and SMF are pumped by 250 mW and 550 mW pump power, respectively. The theoretical gain peak of the individual TDFA and FRA are obtained wavelength of 1460 and 1525 nm region respectively with the maximum gain of 24 dB. The superposition of these gain spectra by the hybrid amplifier has significantly wider the gain bandwidth as shown in Fig. 3. The theoretical gain varies from 20 to 24 dB within a wavelength region from 1460 to 1525 nm, which is in a good agreement with the experimental result obtained by Luthi et al. [11].

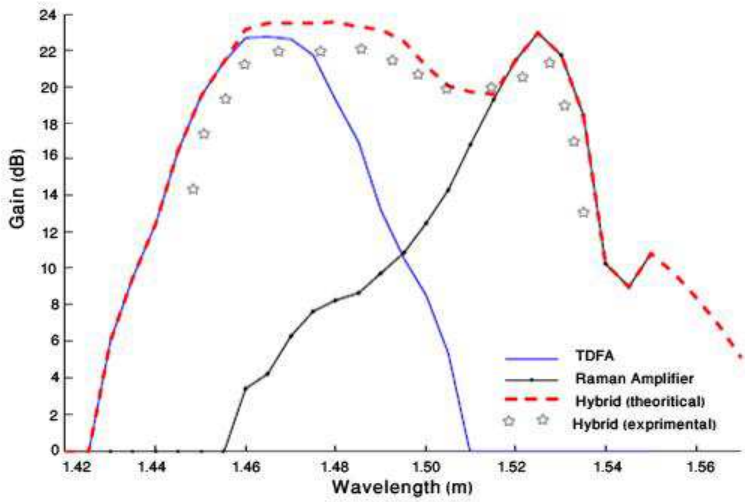

Figure 3. Gain spectra of the TDFA, FRA and the hybrid amplifiers.

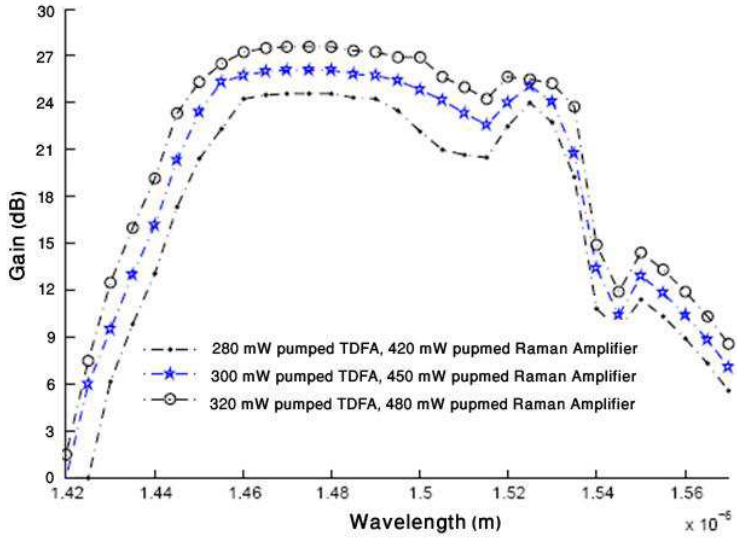

Figure 4. Gain spectra of the hybrid TDFA and Raman amplifier at various pumping powers.

Figure 4 shows the gain spectra obtained in the hybrid amplifier at different total pump powers of 700, 750 and 800 mW. As expected, the gains of the hybrid amplifier increase with the pump power. The gains of the hybrid amplifier peak are obtained at around 24, 25.5 and 27 dB with 700, 750 and 800 mW of pump power, respectively. As seen in the figure, the effect of pump power on TDFA is higher than Raman amplifier and therefore the gain is flattening as the pump power increases.

5. CONCLUSION

The gain characteristic of the hybrid amplifier with a series configuration of TDFA and Raman amplifier is studied. Both gain media of the amplifier uses the same type of pump laser at wavelength of 1420 nm. Cascading of the TDFA and FRA has significantly wider the gain bandwidth. The theoretical gain varies from 20 to 24 dB within a wavelength region from 1460 to 1525 nm, which is in a good agreement with the experimental result. The development of reliable high-power diode lasers in the 1420 nm wavelength range will make this type of wide-band hybrid amplifier an interesting candidate for S-band optical telecommunication systems.

REFERENCES

1. Shahi, S., S. W. Harun, K. Dimyati, and H. Ahmad, "Brillouin fiber laser with significantly reduced gain medium length operating in L-band region," *Progress In Electromagnetics Research Letters*, Vol. 8, 143–149, 2009.
2. Banerjee, A., "New approach to design digitally tunable optical filter system for wavelength selective switching based optical networks," *Progress In Electromagnetics Research Letters*, Vol. 9, 93–100, 2009.
3. Prokopovich, D. V., A. V. Popov, and A. V. Vinogradov, "Analytical and numerical aspects of Bragg fiber design," *Progress In Electromagnetics Research B*, Vol. 6, 361–379, 2008.
4. Mokari, H. and P. Derakhshan-Barjoei, "Numerical analysis of homojunction gallium arsenide avalanche photodiodes (GAAS-APDS)," *Progress In Electromagnetics Research B*, Vol. 7, 159–172, 2008.
5. Moghimi, M. J., H. Ghafoori-Fard, and A. Rostami, "Analysis and design of all-optical switching in apodized and chirped Bragg gratings," *Progress In Electromagnetics Research B*, Vol. 8, 87–102, 2008.
6. Makoui, S., M. Savadi-Oskouei, A. Rostami, and Z. D. Koozehkanani, "Dispersion flattened optical fiber design for large bandwidth and high-speed optical communications using optimization technique," *Progress In Electromagnetics Research B*, Vol. 13, 21–40, 2009.
7. El Mashade, M. B. and M. N. Abdel Aleem, "Analysis of ultrashort pulse propagation in nonlinear optical fiber," *Progress In Electromagnetics Research B*, Vol. 12, 219–241, 2009.
8. Rostami, A. and A. Salmanogli, "Investigation of light amplification in Si-nanocrystal-Er doped optical fiber," *Progress In Electromagnetics Research B*, Vol. 9, 27–51, 2008.
9. Ahmad, H., X. S. Cheng, M. R. Tamjis, and S. W. Harun, "Effects of pumping scheme and double-propagation on the performance of ASE source using dual-stage Bismuth-based Erbium-doped fiber," *Journal of Electromagnetic Waves and Applications*, Vol. 24, No. 2–3, 373–381, 2010.
10. Carena, A., V. Curri, and P. Poggiolini, "Comparison between different configurations of hybrid Raman/Erbium-doped fiber amplifiers," *Proc. Optical Fiber Conference OFC2001*, Vol. 2, TuA3-1 $\sim$ TuA3-3, 2001.
11. Luthi, S. R., G. F. Guimaraes, J. Freitas, and A. Gomes, "TDFA-

FOPA hybrid for S-band amplification and S-to-C, S-to-L band wavelength conversion," *Proc. Quantum Electronics and Laser Science Conference*, 1–2, 2006.

12. Emami, S. D., S. W. Harun, F. Abd-Rahman, H. A. Abdul-Rashid, S. A. Daud, and H. Ahmad, "Optimization of the 1050 nm pump power and fiber length in single-pass and double-pass thulium doped fiber amplifier," *Progress In Electromagnetics Research B*, Vol. 14, 431–448, 2009.
13. Ahmad, H., S. F. Norizan, A. Hamzah, and S. W. Harun, "Double-pass Raman amplifier for gain enhancement and gain clamping," *Optoelectronics and Advanced Materials — Rapid Communication*, Vol. 3, No. 9, 924–926, 2009.
14. Kani, J. and M. Jinno, "Wideband and flat-gain optical amplification from 1460 to 1510 nm by serial combination of a thulium-doped fluoride fibre amplifier and fibre Raman amplifier," *Electronics Lett.*, Vol. 35, No. 12, 1004–1006, 1999.
15. Yam, S. S. H. and J. Kim, "Ground state absorption in thulium-doped fiber amplifier: Experiment and modeling," *IEEE J. Selected Topics in Quantum Electronics*, Vol. 12, No. 4, 797–803, 2006.
16. Peterka, P., B. Faure, W. Blance, and M. Karasek, "Theoretical modeling of S-band thulium doped silica fiber amplifiers," *Optical and Quantum Electron.*, Vol. 36, 201–212, 2004.
17. Headley, G. and P. Agrawal, *Raman Amplification in Fibre Optical Communication Systems*, Elsevier Inc., 2005.
18. Islam, M. N., *Raman Amplifiers for Telecommunications 1: Physical Principles*, Springer, December 2003.
19. Islam, M. N., *Raman Amplifiers for Telecommunications 2: Sub-Systems and Systems*, Springer, December 2003.
20. Yam, S. S. H., J. Kim, M. E. Marhic, Y. Akasaka, and L. G. Kazovsky, "Gain dynamics of 14xx-nm-pumped thulium-doped fiber amplifier," *IEEE Photonics Technology Letters*, Vol. 16, No. 7, 1646–1648, 2004.
21. Desurvire, E., *Erbium-doped Fiber Amplifiers: Principles and Applications*, John Wiley & Sons, New York, 1994.
22. Kasamatsu, T., Y. Yano, and T. Ono, "1.49 μm band gain-shifted thulium doped fiber amplifier for WDM transmission system," *Journal of Lightwave Technol.*, Vol. 20, No. 10, 1826, 1998.